Investigation of the Plasma in a RIT using PIC Modelling

IEPC-2017-518

Presented at the 35th International Electric Propulsion Conference
Georgia Institute of Technology – Atlanta, Georgia – USA
October 8–12, 2017

R. Henrich*, M. Becker† and C. Heiliger‡
Justus Liebig University, Giessen, 35392, Germany

Abstract: A 3D plasma simulation tool is very important for the understanding and optimization of μN-RITs. We have developed a full 3D particle in cell (PIC) code from scratch including electrodynamics called "PlasmaPIC". The simulation tool supports arbitrary geometries which can be imported from a computer aided design (CAD) format. The program is efficiently parallelized up to thousands of cpu cores. In this way the required simulation time can be reduced to only a few hours instead of months. All plasma parameters can be calculated with a very high spatial and temporal resolution. We show simulation results for a μN-RIT 1.0. The results will show that a three dimensional simulation is necessary to cover the coil of the μN-RIT and the extraction system correctly in the simulation.

Nomenclature

$\vec{E}(\vec{r},t)$	= time dependent electric field
$\vec{J}(\vec{r},t)$	= time dependent total current density
$\vec{\tilde{A}}(\vec{r})$	= complex amplitude of the vector potential
$\vec{\tilde{E}}(\vec{r})$	= complex amplitude of the electric field
$\vec{\tilde{J}}(\vec{r})_{coil}$	= complex amplitude of the coil current density
$\vec{\tilde{J}}(\vec{r})_{electrons}$	= complex amplitude of the electron current density
ω	= angular frequency
μ_0	= vacuum permeability
ϵ_0	= dielectric constant
P	= power deposition to plasma
V	= volume occupied by plasma
T	= period of oscillation
μN-RIT	= micro-Newton radio frequency ion thruster
PIC	= Particle in Cell
PIC-MCC	= Particle in Cell - Monte Carlo Collisions
DSMC	= Direct Simulation Monte Carlo
sccm	= standard cubic centimeter per minute
RF	= radio frequency

*Research Scientist, Institute for Theoretical Physics, Robert.Henrich@physik.uni-giessen.de
†PhD Student, Institute for Theoretical Physics, Michael.Becker@physik.uni-giessen.de
‡Professor, Institute for Theoretical Physics, Christian.Heiliger@physik.uni-giessen.de

I. Introduction

Up to date challenging scientific space experiments have high demands, especially in terms of energy consumption, thrust control, and stability of the thruster employed. One of the most promising thruster designs is the μN-RIT (micro-Newton radio frequency ion thruster)[1,2] (figure 1) developed at the University of Giessen. This type uses an inductive plasma discharge which is the key to an extremely long life time. Featured with an extraction grid system for acceleration of the ions enables a high specific impulse for good efficiency. As a matter of fact the μN-RIT fulfills the requirements of a wide range of controllable thrusts with high precision.

Nevertheless, the understanding and optimization of such thrusters is an ongoing process. Besides experiments the plasma modeling is an essential tool for this task. The typical neutral gas pressure in our thruster is in the order of 0.1 Pa. As a consequence, validity of fluid dynamics is not guaranteed for the neutral gas simulation as well as for the plasma simulation and standard commercial tools cannot be used.

To analyze the plasma inside a μN-RIT we have written the simulation program "PlasmaPIC"[3] from scratch. It is based on the "particle in cell" (PIC) method.[4–6] As any other PIC code no assumptions about the plasma are required and all plasma parameters are calculated ab initio with a high spatial and temporal resolution. Even no assumptions about the neutral gas distribution is required in "PlasmaPIC". This is achieved by calculating the neutral gas distribution using the "direct simulation monte carlo" (DSMC) algorithm[7,8] which is self consistently coupled with the PIC algorithm. Nevertheless to minimize the calculation time a homogenous neutral gas distribution which is constant in time can be defined.

Due to the geometry of the thruster, especially the coil and the extraction grid, the thruster symmetries cannot be exploited for the modeling. For this reason we designed "PlasmaPIC" as a full 3D PIC code to describe the inductive coupled plasma discharge. However, the PIC method requires large computational power and thus is rather time consuming. Hence, we massively parallelized our self-developed "PlasmaPIC" simulation tool for all parts of the simulation using MPI. The parallelization performs efficient up to thousands of cpu cores. Due to the 3D design of the code "PlasmaPIC" can handle arbitrary geometries. These geometries can be created with standard CAD tools and can then be imported into our codes.

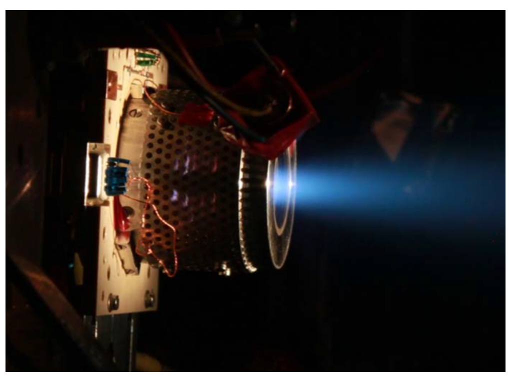

Figure 1: μN-RIT 2.5 (the number indicates the discharge chamber diameter in cm)

II. Electromagnetic Field Modeling in a μN-RIT

The modeling of an inductive coupled plasma discharge, as for our thruster, requires an electrodynamic treatment. Due to the necessity of resolving the speed of light such a fully electrodynamic treatment is computationally too expensive. Assuming that the electromagnetic field and current densities are varying harmonically in time the field solver can be split into an electrostatic part and an electromagnetic part[9–11]. The electrostatic part consist of a PIC-MCC algorithm written in an objected-oriented[12] manner with c++. The MCC[13] part includes for the collisions of the electrons with the neutral gas the elastic scattering, excitation, and ionization. For the collisions of the ions with the neutral gas the elastic scattering and charge-exchange collisions are incorporated. For advancing the charged particles the leap-frog method[7] is applied. Furthermore, the ions and electrons can be moved on different time scales. Within the electrostatic part the Poisson equation has to be solved at each time step. This is done by the finite difference method

Successive over Relaxation (SOR). Implemented boundary conditions are Dirichlet for equipotential objects and Neumann for floating and current-driven objects.[14, 15] Additionally, dielectric objects can be defined with different relative permittivities[15] and different secondary electron emission coefficients. Each of these boundary conditions is only implemented in the electrostatic part.

For the electrodynamic part the wave equation

$$\Delta\vec{E}\left(\vec{r},t\right)=\mu_0\frac{\partial}{\partial t}\vec{E}\left(\vec{r},t\right). \tag{1}$$

has to be solved which is derived from the Maxwell's equations by neglecting the displacement current and assuming that electrostatic fields in the plasma are negligible.

By expressing the time varying electric field $\vec{E}(\vec{r},t)$ by a complex amplitude $\tilde{\vec{E}}(\vec{r})$ and the applied frequency ω of the coil current $\tilde{J}_{coil}$, the time dependent part can be separated as

$$\vec{E}\left(\vec{r},t\right)=\tilde{\vec{E}}\left(\vec{r}\right)e^{i\omega t}. \tag{2}$$

Telegrapher's equation then takes on the form

$$\Delta\tilde{\vec{E}}(\vec{r})=i\omega\left(\tilde{\vec{J}}(\vec{r})_{coil}+\tilde{\vec{J}}(\vec{r})_{electrons}\right), \tag{3}$$

whereas the complex amplitude of the electron current density is derived by a discrete Fourier transformation of the electron velocity. This is carried out each time step for the driven frequency of the coil and averaged over one rf cycle. At this the ion current density can be neglected because the ions are barely influenced by the electric field of the coil due their large mass. That separation is very convenient in the way that now this equation has not to be solved every time step to obtain the electric field. It is sufficient to calculate the electric field at every RF cycle. As a consequence, the computational effort is dramatically reduced. The system of equations (eq.3) can be separated in six equations, real and imaginary part for each of the three space components. Each equation can be solved independently by applying the same field solver as for the Poisson equation The boundary conditions for the complex electric field amplitude are given by the definition of the vector potential $\vec{A}$ and the Biot-Savarts law

$$\tilde{\vec{E}}(\vec{r},t)=-\frac{\partial}{\partial t}\tilde{\vec{A}}(\vec{r},t) \tag{4}$$

$$\tilde{\vec{E}}(\vec{r})=-i\omega\tilde{\vec{A}}(\vec{r})=-i\omega\frac{\mu_0}{4\pi}\int d^3r'\,\frac{\left(\tilde{\vec{J}}(\vec{r})_{coil}+\tilde{\vec{J}}(\vec{r})_{electrons}\right)}{\left|\vec{r}-\vec{r'}\right|}. \tag{5}$$

Using equation 5 the electric field amplitude at every grid point located at the border of the simulation area is calculated. All other inner grid points are derived by solving equation 3. For the electromagnetic part no further boundary conditions are included up to now.

In "PlasmaPIC" the power deposition is a predefined target value. The actual achieved power deposition P is averaged over the time T of one RF cycle and is calculated from

$$P=\frac{1}{T}\int\limits_T\int\limits_V\vec{J}(\vec{r},t)\cdot\vec{E}(\vec{r},t)\mathrm{d}^3r\mathrm{d}t. \tag{6}$$

The coil current will be readjusted at every RF cycle until the actual achieved power deposition matches the predefined target value.

III. Simulation of a μN-RIT 1.0

We applied our 3D PIC code "PlasmaPIC" to a μN-RIT 1.0. We chose the small diameter of 1 cm for testing purposes and to keep the computational effort reasonable. For a μN-RIT 2.5 the system size will increase by a factor of 2.5 in every direction. Assuming the same plasma density and electron temperature for a μN-RIT 2.5 the cell size can be kept constant. Accordingly, the number of required cells in every direction for this simulation will also increase by a factor of 2.5. Consequently, the total number of cells will

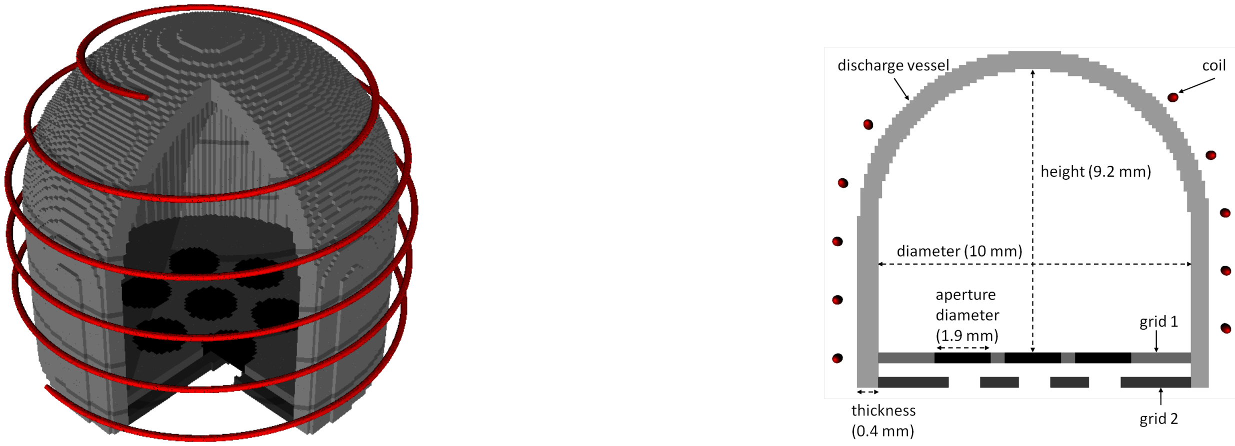

Figure 2: Three dimensional overview (left) and two dimensional schematic (right) of the used μN-RIT 1.0 in "PlasmaPIC"

increase by a factor of about 15 as well as the number of particles. For that reason the total simulation time will increase at least by a factor of 15.

The imported geometry was designed with a CAD program and is shown in figure 2.

It shows the coil (red) spirally surrounding the discharge chamber (light gray) and the two extraction grids (dark gray). The diameter of the discharge vessel is 10 mm and the inner height is 9 mm. The diameter of the apertures in the first grid is 1.9 mm. The simulation area for the electromagnetic fields is the smallest cuboid which encloses the discharge chamber. In contrast, the plasma region is limited to the area enclosed by the discharge chamber and the first grid. At the first grid 1500 V and at the second grid 0 V are applied. Additionally, the potential on the surface of the discharge chamber is fixed to 1500 V due to a better calculation performance. The apertures of first grid are filled with exit planes to remove the extracted ions from the simulation. The working gas is Xenon. The used input parameter for the power deposition is 0.08 watt. The coil consists of five turns and operates at a frequency of 5 MHz. The neutral gas density is at at $2 \cdot 10^{20}$ particles per cubic meter. Furthermore, the neutral gas distribution is assumed to be homogeneous in space and constant in time. The used mesh size for this simulation is $100 \times 100 \times 100$ and the amount of particles totals up to 23 million. The simulation was done by 384 cores in 24 hours. The cell size is set to 0.11 mm in each direction and the time step is set to $7.5 \cdot 10^{-12}$ s.

After 0.8 million time steps the simulation has reached the steady state. This corresponds to a simulation time of 6 μs respectively 30 rf cycles. Figures 3 and 4 show the electron and ion density distribution for the steady state. The slight asymmetry in both distributions is due to the slope of the coil and can only be observed with a three dimensional simulation.

The average electron density is about 6 eV and the spatial distribution is shown in figure 5. As it can be seen the energy is obviously higher near the coil due to the fact that the electric field has its maximum at the coil and drops to zero in the middle of the discharge chamber because of its rotationally field character. The magnitude of the electric field amplitude is shown in figure 7. In accordance to this the power deposition is larger in the vicinity of the coil and vanishes to middle of the discharge chamber which is shown in figure8. The asymmetric electric field of the coil leads to the simulated asymmetric character of the spatial electron energy distribution and underlines the importance of a 3D simulation.

The electric potential is shown in figure 6. It can be seen that the plasma is biased to 1500 V by the first grid. The plasma potential is at 26 eV. The white area above the first grid is related to the fact, that the potential there is lower than 1500 eV due to the voltage of the second grid which is 0 V. On this account electrons have not enough energy to overcome the potential above the first grid in the region of the extraction channels. Thus no electrons can get there and hence the same region is also white in figure 5. The ion energy is shown in 9. It can be seen that the energy of the ions is at room temperature only in the middle of the discharge chamber and hence the plasma bulk is quite small. In contrast the plasma pre sheath is very large and covers the most part of the discharge chamber.

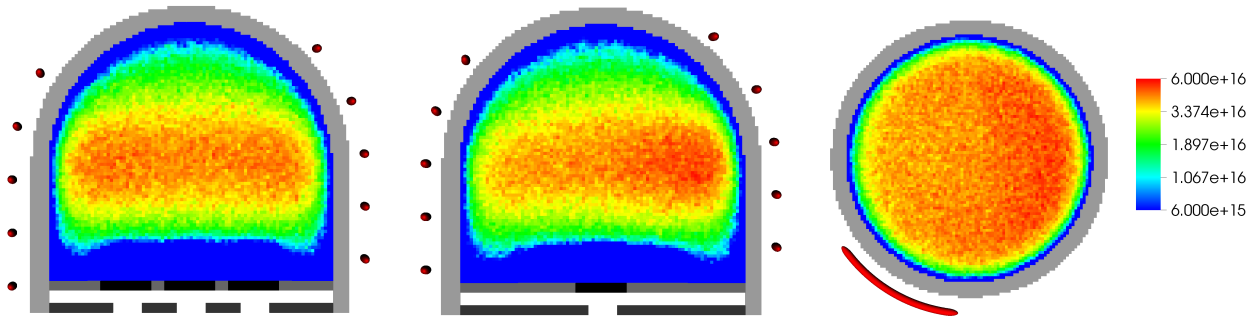

Figure 3: Electron density in $1/m^3$ for a μN-RIT 1.0: x-z plane (left), y-z plane (middle) and x-y plane at position 4 mm above grid 1 (right)

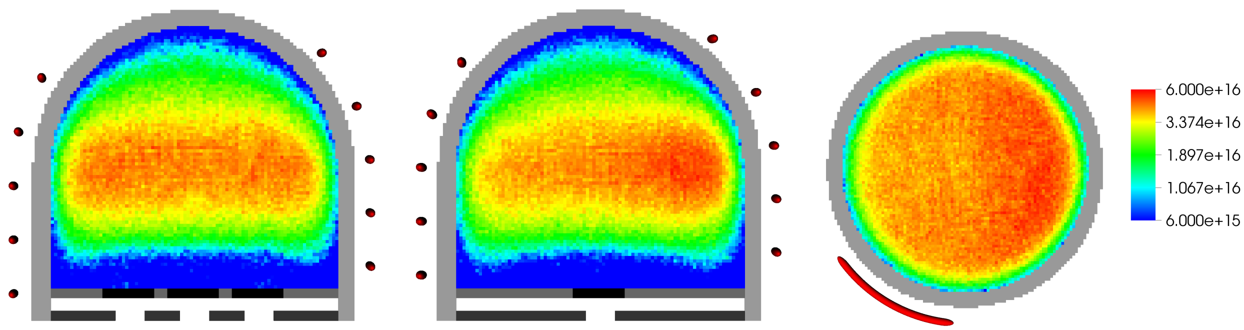

Figure 4: Ion density in $1/m^3$ for a μN-RIT 1.0: x-z plane (left), y-z plane (middle) and x-y plane at position 4 mm above grid 1 (right)

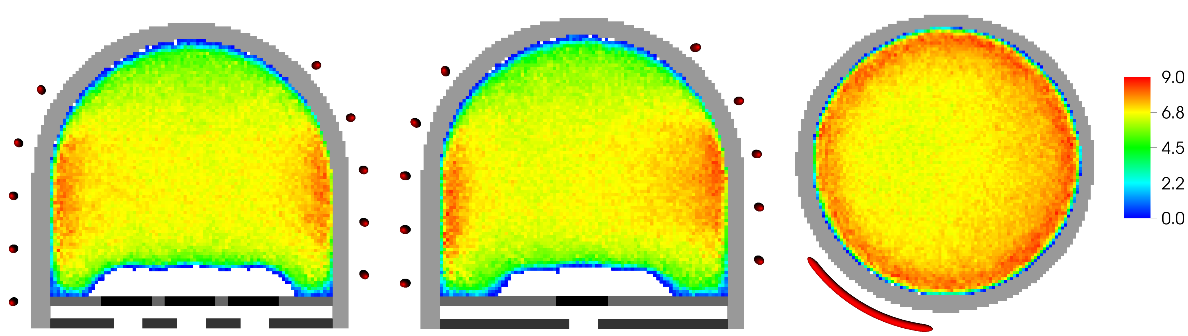

Figure 5: Electron energy in eV for a μN-RIT 1.0: x-z plane (left), y-z plane (middle) and x-y plane at position 4 mm above grid 1 (right)

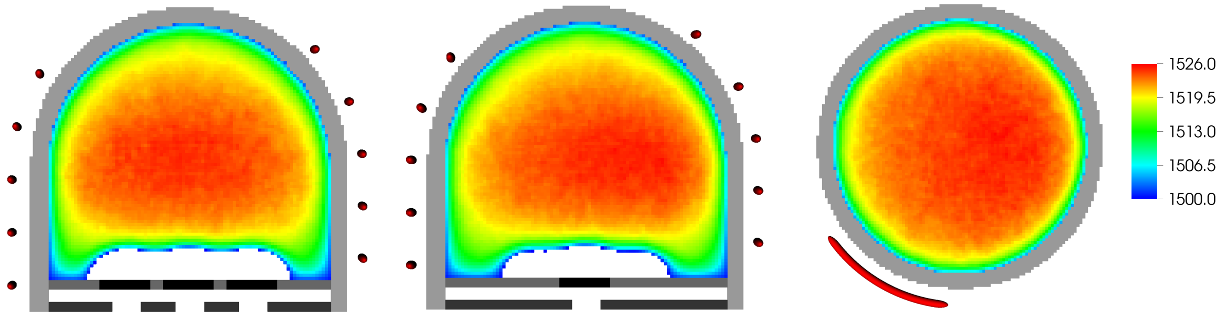

Figure 6: Electric potential in V for a μN-RIT 1.0: x-z plane (left), y-z plane (middle) and x-y plane at position 4 mm above grid 1 (right)

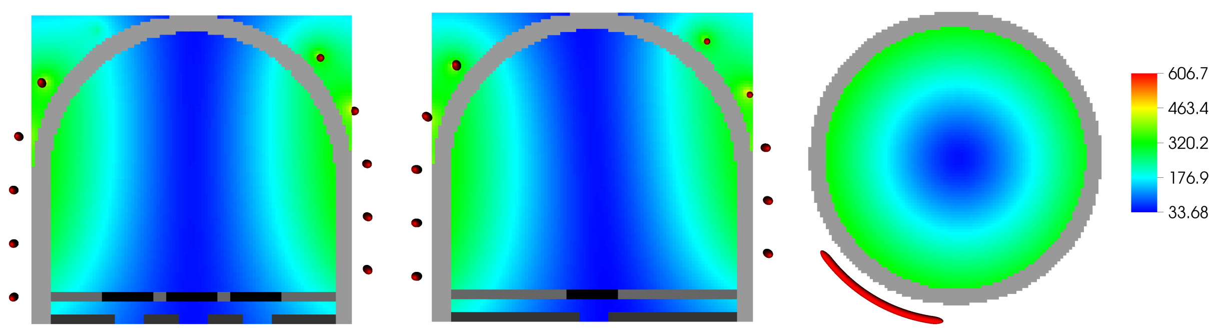

Figure 7: Magnitude of the electric field amplitude of the coil in V/m for a μN-RIT 1.0: x-z plane (left), y-z plane (middle) and x-y plane at position 4 mm above grid 1 (right)

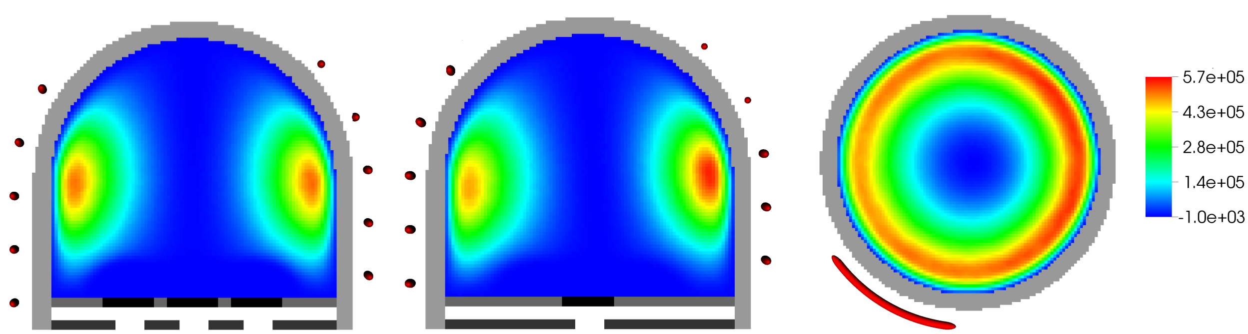

Figure 8: Power deposition in W/m^3 for a μN-RIT 1.0: x-z plane (left), y-z plane (middle) and x-y plane at position 4 mm above grid 1 (right)

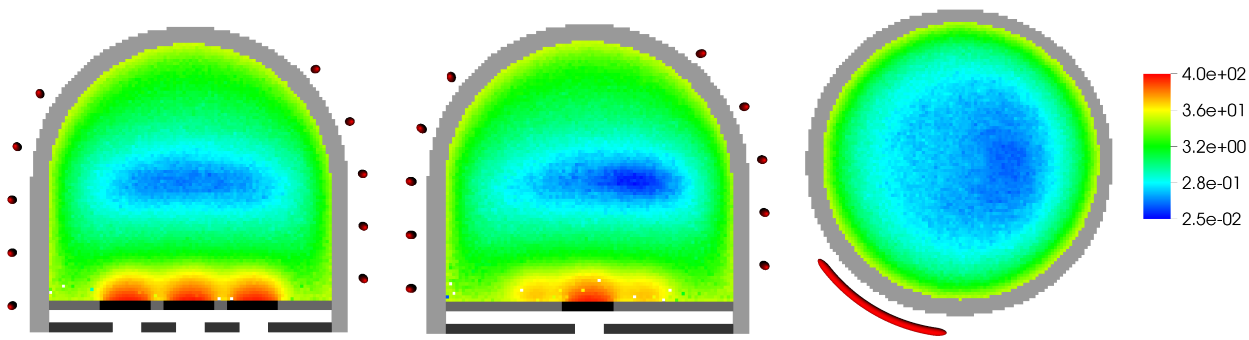

Figure 9: Ion energy in eV for a μN-RIT 1.0: x-z plane (left), y-z plane (middle) and x-y plane at position 4 mm above grid 1 (right)

IV. Conclusion

We are now able to perform 3D plasma simulations for μN-RIT's. Our self-developed simulation code "PlasmaPIC" supports arbitrary geometries, which can be easily designed by standard CAD tools. All parts of "PlasmaPIC" are parallelized. The parallelization is efficient up to thousands of cpu cores. Thus, the calculation time reduces from months to only a few days or hours depending on the amount of available cores. We have shown that a three dimensional plasma simulation reveals slight asymmetries in the density distributions. Our next steps will be the increase of the system size and thus we will be entering the verification phase. We are now on the verge of predicting performance parameters for new designs of our thrusters on a microscopic level.

References

[1]Horst W. Loeb, K.-H. Schartner, Stefan Weis, Davar Feili, and Bruno K. Meyer. Development of rit_microthrusters. In *55th International Astronautical Congress*, 2004.

[2]Davar Feili, Davina M. Di Cara, Hans J. Leiter, Jose G. Del Amo, Horst W. Loeb, Stefan Weis, Danny Kirmse, Hans Müller, and Bruno K. Meyer. The μNRIT-4 ion engine: a first step towards a european mini-ion engine system development. In *The 30th International Electric Propulsion Conference*, 2007.

[3]Robert Henrich. *Development of a Plasma Simulation Tool for Radio Frequency Ion Thrusters*. PhD thesis, Justus-Liebig-Universität Gießen, 2013.

[4]A. B. Langdon C. K. Birdsall. *Plasma Physics via Computer Simulation*. Taylor and Francis, 2005.

[5]Roger W. Hockney and J. W. Eastwood. *Computer Simulation Using Particles*. Inst of Physics Pub, 1988.

[6]D. Tskhakaya, K. Matyash, R. Schneider, and F. Taccogna. The particle-in-cell method. *Contributions to Plasma Physics*, 47(8-9):563–594, 2007.

[7]G.A.Bird. *Molecular Gas Dynamics and the Direct Simulation of Gas Flows*. Oxford Science Publications, 1994.

[8]Francis J. Alexander and Alejandro L. Garcia. The direct simulation monte carlo method. *Computers in Physics*, 11(6), 1997.

[9]Benjamin W. Yu and Steven L. Girshick. Modeling inductively coupled plasmas: The coil current boundary condition. *Journal of Applied Physics*, 69(2):656–661, 1991.

[10]K.-I. You and N. S. Yoon. Discharge impedance of solenoidal inductively coupled plasma discharge. *Phys. Rev. E*, 59:7074–7084, Jun 1999.

[11]Yoshinori Takao, Naoki Kusaba, Koji Eriguchi, and Kouichi Ono. Two-dimensional particle-in-cell monte carlo simulation of a miniature inductively coupled plasma source. *Journal of Applied Physics*, 108(9):093309, 2010.

[12]N.T. Gladd J.P. Verboncoeur, A.B. Langdon. An object-oriented electromagnetic pic code. *Computer Physics Communications*, 87:199–211, 1995.

[13]V. Vahedi and M. Surendra. A monte carlo collision model for the particle-in-cell method: applications to argon and oxygen discharges. *Computer Physics Communications*, 87(1-2):179–198, 1995. ¡ce:title¿Particle Simulation Methods¡/ce:title¿.

[14]J.P. Verboncoeur, M.V. Alves, V. Vahedi, and C.K. Birdsall. Simultaneous potential and circuit solution for 1d bounded plasma particle simulation codes. *Journal of Computational Physics*, 104:321–328, 1993.

[15]Vahid Vahedi and G. DiPeso. Simultaneous potential and circuit solution for two-dimensional bounded plasma simulation codes. *J. Comput. Phys.*, 131:JOURNAL OF COMPUTATIONAL PHYSICS, 1997.

Acknowledgments

This work has been supported by the "Bundesministerium fuer Wirtschaft und Energie". Grant 50RS1507